Biochemical and Biophysical Research Communications 391 (2010) 248–253

Contents lists available at ScienceDirect

Biochemical and Biophysical Research Communications

journal homepage: www.elsevier.com/locate/ybbrc

GD3–7-aldehyde is an apoptosis inducer and interacts with adenine nucleotide translocase

Catherine Brenner [a,1], Bernhard Kniep [b,1,*], Evelyne Maillier [a], Cécile Martel [a], Claudia Franke [b], Nadja Röber [b], Michael Bachmann [b], Ernst Peter Rieber [b], Roger Sandhoff [c]

[a] University of Versailles-SQY, PRES UniverSud Paris, CNRS UMR8159, 45, Avenue des Etats-Unis, 78035 Versailles, France
[b] Technical University of Dresden, Institute of Immunology, Medical Faculty Carl Gustav Carus, Fetscherstr. 74, 01307 Dresden, Germany
[c] German Cancer Research Center, Department of Cellular and Molecular Pathology, Im Neuenheimer Feld 280, 69120 Heidelberg, Germany

ARTICLE INFO

Article history:
Received 31 October 2009
Available online 11 November 2009

Keywords:
Apoptosis
Adenine nucleotide translocase
GD3
GD3–7-aldehyde

ABSTRACT

We prepared GD3–7-aldehyde (GD3–7) and determined its apoptotic potential. GD3–7 proved to be more efficient to induce pro-apoptotic mitochondrial alterations than GD3 when tested on mouse liver mitochondria. GD3–7-induced mitochondrial swelling and depolarization was blocked by cyclosporin A (CsA) supporting a critical role of the permeability transition pore complex (PTPC) during GD3–7-mediated apoptosis. In contrast to GD3, GD3–7 was able to induce channel formation in proteoliposomes containing adenine nucleotide translocase (ANT). This suggests that ANT is the molecular target of GD3–7. Using a specific antiserum, GD3–7 was detected in the lipid extract of the myeloid tumor cell line HL-60 after apoptosis induction, but not in living cells. Therefore, GD3–7 might be a novel mediator of PTPC-dependent apoptosis in cancer cells.

Introduction

Intracellular GD3 formation is a consequence of pro-apoptotic signals induced by FAS/FASL [1], TNF-α [2] and β-amyloid [3]. It has various effects such as production of reactive oxygen species (ROS) [4], opening of a mitochondrial multiprotein complex, the permeability transition pore complex (PTPC) [4], release of cytochrome *C* from mitochondria [1], activation of caspases [5], and inhibition of the translocation of NFκB into the nucleus [6]. Apoptosis mediated by GD3 can be blocked by CsA and by the oncoprotein Bcl-2, two inhibitors of the PTPC-dependent permeability transition (PT) [7,8], which underlines the important role of mitochondria in the signalling of GD3-induced apoptosis. The GD3 effect is suppressed by antioxidants [9]. This suggests that GD3 oxidation may be critical for apoptosis induction. In cells, especially in certain types of tumors GD3 is frequently found along with a derivative that is 9-*O*-acetylated at the terminal sialic acid yielding 9-*O*-acetyl GD3 (acGD3) [10–12]. AcGD3 is able to suppress the pro-apoptotic effect of GD3 [13]. While 9-*O*-acetylation probably has only a limited effect on the hydrophobicity or steric conformation of GD3, it was found to block the oxidative modification of GD3 thus preventing the formation of oxidized GD3 variants [14]. The aims of this study were to compare the impact of GD3 and its derivatives for the regulation of apoptosis. We prepared GD3–7-aldehyde (GD3–7) as a highly effective pro-apoptotic variant of GD3 and addressed the question of ANT as its mitochondrial target. In addition we demonstrated the formation of GD3–7 in the human tumoral cell line HL-60 after apoptosis induction.

Materials and methods

Cell culture and induction of apoptosis. When not indicated otherwise, chemicals were from Sigma (St. Louis, MO). HL-60 cells were obtained from the Department of Immunology, University of Munich, Germany. They were maintained at a concentration of <1 × 10^6 cells/ml in RPMI 1640 medium containing 5% heat-inactivated fetal bovine serum, 100 U/ml penicillin G, 100 μg/ml streptomycin, and 2 mM glutamine. To induce apoptosis a 10 mM solution of C2-ceramide in dimethyl sulfoxide (DMSO) (Merck, Darmstadt, Germany) was added directly to cell suspensions to obtain the indicated concentrations for a 24 h culture.

Abbreviations: amu, atomic mass units; ANT, adenine nucleotide translocase; CAT, carboxyatractyloside; CsA, cyclosporin A; CypD, cyclophilin D; $\Delta\Psi_m$, mitochondrial transmembrane potential; MMP, mitochondrial membrane permeabilization; PT, permeabilty transition; PTPC, permeability transition pore complex; VDAC, voltage-dependent anion channel; 4-MUP, 4-methyl umbelliferyl phosphate; GM3, II^3NeuAc-LacCer; GD3, $II^3(NeuAc)_2$-LacCer; GD3–7, GD3–7-aldehyde; AcGD3, 9-*O*-acetyl GD3.

* Corresponding author. Address: Alttolkewitz 14, 01279 Dresden, Germany. Fax: +49 351 458 6316.
E-mail address: ekniep@t-online.de (B. Kniep).

[1] Both authors contributed equally to this work.

0006-291X/$ - see front matter © 2009 Elsevier Inc. All rights reserved.
doi:10.1016/j.bbrc.2009.11.044

The extent of apoptosis was measured using the method of Nicoletti et al. [15].

Gangliosides. GD3 and acGD3 were purified from bovine buttermilk and characterized as described [16]. Oxidized GD3 was prepared as follows: 2 mg GD3 was sonicated in 2 ml of 100 mM sodium acetate buffer pH 5.5 in an ultrasonic bath for 15 min at 0 °C. The solution was then mixed with 2 ml of 10 mM sodium periodate in the same buffer and incubated in the dark at 0 °C for 2 h. Excess sodium periodate was removed by incubation with 2 ml of 50% glycerol at 0 °C for 20 min. The incubation mixture was then dialyzed at 4 °C and dried. HPTLC resulted in a single band. The oxidized ganglioside was analyzed by NanoESI-MS/MS mass spectrometry.

MS/MS mass spectrometry. NanoESI-MS/MS-analysis was performed with a triple quadrupole instrument [VG micromass (Cheshire, UK) model Quattro II] equipped with a nano-electrospray source and gold-sputtered capillaries as described [17,18]. Parameters for cone voltage and collision energy of the different scan-modes are listed in Supplemental Table 1.

Ganglioside analysis. $3–20 \times 10^7$ cells were extracted successively with 5 ml each of methanol, chloroform–methanol (1:2, v/v), and chloroform–methanol (2:1, v/v) in an ultrasonic bath (5 min in ice cold water). The combined solvent extracts were evaporated at 25 °C under reduced pressure. The residue was homogenized in 5 ml of 0.88% aqueous KCl in an ultrasonic bath and desalted on a glass column filled with 600 mg Sep-Pak C18 coated 55–105 μm silica particles (Waters, Milford, MA, USA) as described [19]. The desalted lipids were separated on silica 60 HPTLC plates (Merck, Darmstadt, Germany), (solvent: chloroform–methanol–water (120:70:17, v/v/v), containing 0.02% (w/v) $CaCl_2$) and were immunostained as described [20,21]. Gangliosides were quantified by densitometry of the HPTLC plates with a Shimadzu PC 9000 scanner at 580 nm using orcinol staining and quantified standards.

Isolation of mouse liver mitochondria. Mitochondria were isolated from mouse liver (Balb/c, female, 6–8 weeks old, Charles River, l'Arbresle, France) by differential centrifugations and purified on Percoll gradient [22]. Protein concentration was determined using the micro-BCA assay (Pierce Chemical Company, Rockford, Illinois).

Monoclonal antibodies and preparation of GD3–7-specific antiserum. A culture supernatant of the GD3-specific monoclonal antibody (mAb) R24 (CD60a) was a kind gift from Johannes Müthing, Münster, Germany. For preparation of a GD3–7-specific antiserum, 2 Balb/c × C3H/F1 mice (Charles River, Sulzfeld, Germany) were immunized intraperitoneally with an emulsion of 50 μg purified GD3–7 in sterile physiological NaCl in complete Freunds adjuvant. After four injections in 3-week intervals, the serum was tested at a 1:100 dilution for GD3–7 and GD3 immunoreactivity using TLC immunostaining. The serum, named anti-GD3–7, reacted strongly with GD3–7 but not with GD3 and other non-oxidized gangliosides from human leukocytes.

Swelling and depolarization assays. For swelling and depolarization measurements, mitochondria (25 μg protein) were diluted in a hypo-osmotic buffer (10 mM Tris–MOPS, 5 mM succinate, 200 mM sucrose, 1 mM phosphate, 10 μM EGTA, and 2 μM rotenone, pH 7.4) and distributed into 96-well microtiter plates (200 μl/well). After addition of various doses of calcium (Ca^{2+}), carboxyatractyloside (CAT), GD3, GD3–7, and acGD3, the mitochondrial swelling was immediately measured by the decrease in absorbance at 540 nm for 1000 s. The depolarization of the mitochondria was measured concomitantly by the rhodamine 123 fluorescence dequenching assay (1 μM, λ_{exc}: 485 nm, λ_{em}: 535 nm, Molecular Probes). Both assays were adapted from [23,24] and were performed at 37 °C in a spectrofluorimeter (TECAN Genios, TECAN, Grödig, Austria).

PTPC purification and reconstitution into liposomes. The PTPC was purified from four rat brains (Wistar rats, male, 11–12 weeks old, Charles River) and reconstituted into cholesterol: phosphatidylcholine (1:50 w/w) liposomes [25,26]. The ability of GD3 and derivatives to activate the pore function of PTPC was evaluated by addition of alkaline phosphatase (which converts 4-methylumbelliferylphosphate (4-MUP) into the fluorochrome 4-methylumbelliferone) to measure the release of entrapped 4-MUP in comparison to calcium induced 4-MUP release [22]. The 100% of 4-MUP release was determined by adding 0.5 mM Ca^{2+} to proteoliposomes. The fraction enriched in the PTPC components, which was used for the reconstitution into liposomes was analyzed for the presence of ANT, voltage-dependent anion channel (VDAC) and cyclophilin D (CypD) by sodium dodecylsulfate–polyacrylamide gel electrophoresis (SDS–PAGE, 12%) and Western-blotting with a rabbit polyclonal serum against ANT (Genosphere, Paris, France), a rabbit polyclonal serum against VDAC (Genosphere, Paris, France), and a monoclonal antibody against CypD (Mitosciences, Eugene, Oregon).

ANT purification and reconstitution into liposomes. ANT was purified from rat heart mitochondria [22], checked to be VDAC and CypD-free, and reconstituted into proteoliposomes (phosphatidylcholin/cardiolipin (45:1, w/w)). Proteoliposomes were loaded either with 4-MUP in 10 mM KCl, 10 mM Hepes, 125 mM saccharose (pH 7.4), by sonication, washed on PD10 columns, dispensed in 96-well microtiter plates and incubated with the indicated agents at 20 °C. The release of 4-MUP was quantified by addition of alkaline phosphatase. The 100% of 4-MUP release was determined by adding 1 μM CAT to proteoliposomes. The fluorescence induced by the treatment of liposomes by another agent was calculated as a percentage of CAT-induced 4-MUP release.

Results

To test our hypothesis that the oxidation of GD3 is required for its pro-apoptotic function it was subjected to mild periodate oxidation and the effects of the oxidized and of the unchanged GD3 and of acGD3 on the PTPC and ANT function were compared. The purified oxidized GD3 was analyzed by nanoESI-MS/MS. Fragmentation of the oxidized GD3 revealed a characteristic fragment of m/z −519 instead of m/z −581, the latter being characteristic for the two linked sialic acids in GD3 (Fig. 1A and B). The difference represents a loss of 62 amu corresponding to $C_2H_6O_2$. This fits only with the 7-aldehyde but not the 8-aldehyde form of GD3. The loss of 62 amu is due to a breakdown of the terminal sialo-group as single-charged fragments corresponding to GM3, LacCer, GlcCer, and Cer are unchanged in comparison to corresponding GD3 spectra. For measurement samples were dissolved in methanol. Aldehydes easily form hemiacetals with alcohols. Hence, methanoyl-GD3–7 hemiacetals were also present and their fragmentation spectra revealed a fragment due to the loss of methanol (32/2 amu/e) but were otherwise very similar to GD3–7 fragmentation spectra (data are only shown for the species containing the Cer(d18:1, 22:0) lipid anchor, Fig. 1A–C).

The oxidation products of GD3 turned out to be exclusively GD3–7 as all ganglioside molecules detected with a general scan for sialic acids (m/z −87) were also identified with the fragment m/z −519, specific for GD3–7 and no signals corresponding to the molecular weights of educt GD3-species were found (Fig. 1D and E), also not with a scan for the two intact sialic acids (m/z −581) (data not shown). Scanning the oxidized GD3 sample with the neutral loss of 16 amu, the subset of methanoyl-hemiacetals was

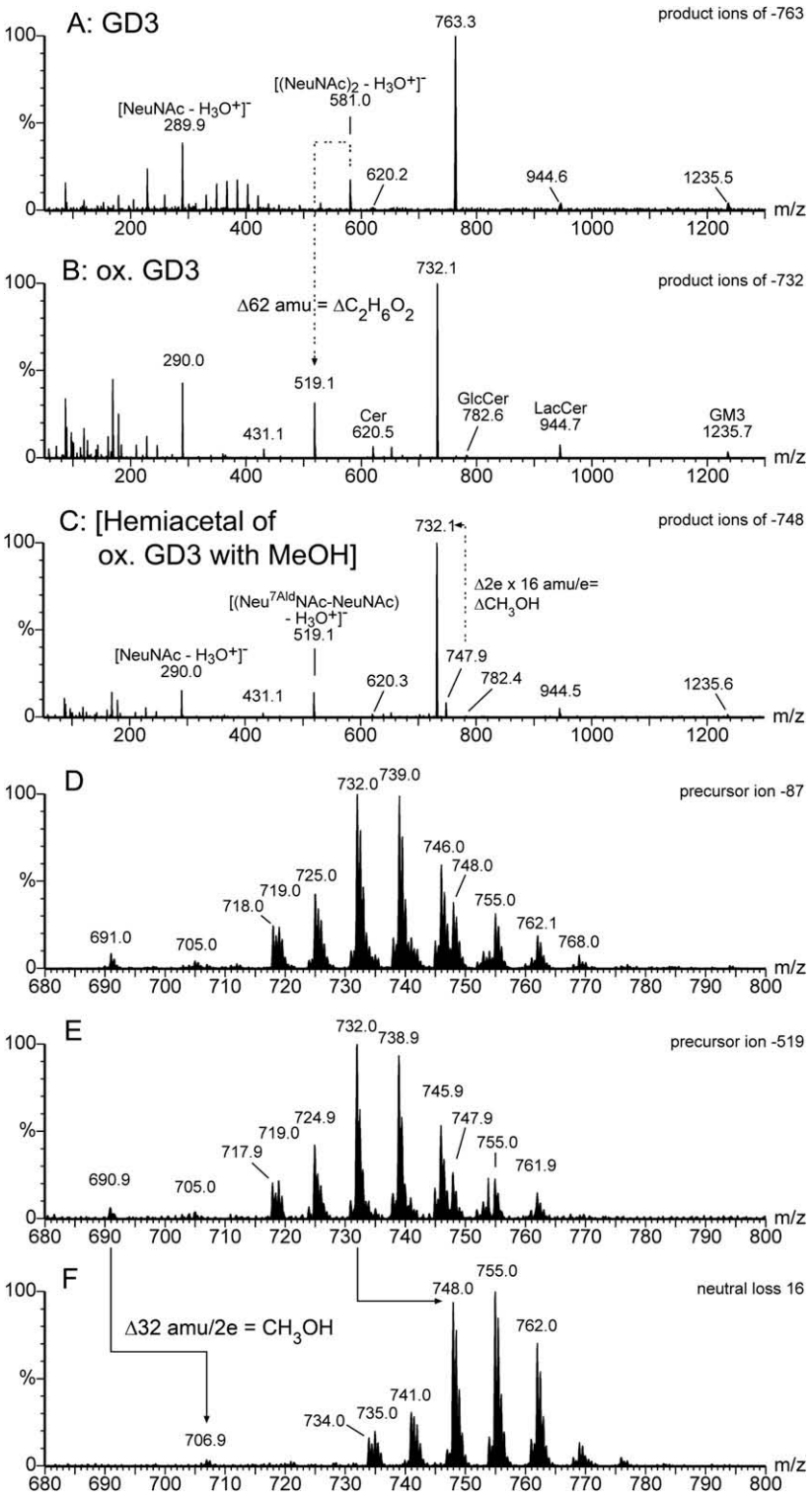

Fig. 1. Detection of purified GD3–7 by tandem-mass spectrometry and representative product ion spectra of GD3, GD3–7 and the methanoyl-hemiacetal of GD3–7. (A) Precursor ion *m/z* −87 spectrum showing all gangliosides with the measured *m/z* range. *Note:* no signals corresponding to GD3 are visible. (B) Precursor ion *m/z* −519 spectrum: As shown in Fig. 3, the fragment *m/z* −519 is specific for GD3–7 but not GD3. *Note:* all signals seen in (A) are detectable in (B) and represent the GD3–7. (C) Neutral loss *m/z* 16 corresponding to the loss of methanol from double-charged compounds. *Note:* signals found in (C) are present in (A) and (B) as minor pattern and corresponds by a shift of −16 amu/e exactly to the major pattern. Therefore, all GD3–7 species are also present as GD3–7-methanoyl-hemiacetals making up roughly 20% of the aldehyde. (D) Product ions of GD3 (d18:1, 22:0). At low collision energy (27 eV) not only the fragment for sialic acid at *m/z* -290 but also the signal at *m/z* 581 characteristic for a single-charged disialo-group is abundant. Fragmentation of the double-charged GD3-molecules allows the detection of single-charged fragments corresponding to GM3, LacCer, GlcCer, and Cer. (E) Product ions of GD3–7 (d18:1, 22:0). No fragment at *m/z* 581 is detectable showing structural changes in the disialo-group. A new single-charged fragment (*m/z* 519) smaller by 62 amu/e is found, fitting to a single-charged disialo-group that has been oxidized at one sialo-group to the 7-aldehyde. This fragment was found in all product ion spectra of the GD3–7 species detected (Fig. 2A and B). Fragments for GM3, LacCer, GlcCer and Cer have identical *m/z* values as GD3 (d18:1, 22:0) in (A) by that demonstrating that the loss of 62 amu is due to oxidation of the outer NeuNAc and leaving the core GM3-structure unchanged. (F) Product ions of GD3–7-methanoyl-hemiacetal (d18:1, 22:0). After loss of 16 amu/e the spectrum is very similar to that of (B). Therefore the compound with *m/z* 748 very likely represents an adduct of the 7-aldehyde *m/z* 732. Taking the two charges into account, the adduct has a molecular weight of 32 amu, the molecular weight of methanol.

detected (Fig. 1F). Their pattern fits after subtraction of 16 amu/e to the residual patterns found with the precursor ion scans −87 and −519. Compositions of the various GD3–7 species are found in the supplemental data.

To compare the mitochondrial effects of GD3, acGD3, and GD3–7, we isolated mouse liver mitochondria and evaluated the effects of the various GD3 derivatives on the volume of mitochondria (Fig. 2A) and on their transmembrane inner potential ($\Delta\Psi_m$) (Fig. 2B). We found that GD3 and GD3–7 can directly induce a partial matrix swelling (Fig. 2A). Both molecules were less efficient than Ca^{2+}, the prototypic inducer of mitochondrial permeability transition (PT) and than CAT, a PT inducer that targets ANT. GD3–7 proved to be more potent than GD3. In contrast, acGD3 was inactive (Fig. 2A). The mitochondrial depolarization by GD3 and GD3–7 was maximal and similar to Ca^{2+} and CAT (Fig. 2B). As previously reported for GD3, the induction of mitochondrial swelling and depolarization of GD3–7 were inhibited by CsA indicating that the process is mediated by the PTPC (results not shown).

Thereafter, we decided to identify the target of GD3 derivatives in mitochondria. To that end, we purified and reconstituted PTPC into liposomes as previously described [25]. The protocol leads to proteoliposomes highly enriched in VDAC, ANT and CypD, which are candidate proteins for PTPC [27–29]. Their presence in the proteoliposomes is shown in Fig. 3A. The proteoliposomes were briefly sonicated to encapsulate the fluorescent probe 4-MUP and KCl to generate a diffusion gradient [22]. After treatment with Ca^{2+}, we detected a dose-dependent increase in fluorescence correlating with a probe release through open pores of the PTPC (Fig. 3B). Comparatively, GD3–7 was able to induce a partial release of 4-MUP (Fig. 3C). This effect was dependent on the reconstitution of PTPC proteins, since GD3–7 was inactive on pure lipidic liposomes of the same composition (i.e. phosphatidylcholine:cholesterol), but devoid of proteins (not shown). GD3 and acGD3 were not able to induce the pore opening of PTPC (Fig. 3C).

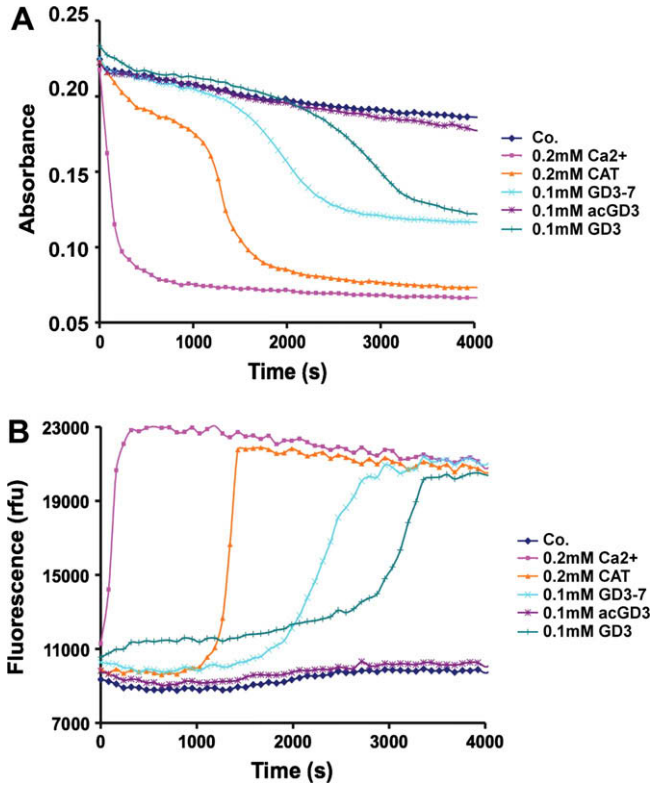

Fig. 2. Effects of GD3 and its derivatives in mitochondria. (A) Induction of swelling. Isolated mitochondria (25 μg protein/well) were treated with Ca^{2+}, CAT, GD3–7, acGD3, GD3, or not (Co.) at 37 °C and the absorbance at 540 nm was recorded for 4000 s to measure the swelling of the mitochondrial matrix. (B) Induction of the transmembrane inner potential ($\Delta\Psi_m$) depolarization. Isolated mitochondria were treated in the same conditions as in A in the presence of a $\Delta\Psi_m$-sensitive probe, Rh123, and the fluorescence was recorded for 4000 s.

These results prompted us to evaluate the effect of GD3–7 on ANT-liposomes to determine whether ANT could be a target of GD3–7. We purified ANT from rat heart to homogeneity in a form free of contaminants such as VDAC or CypD (Fig. 3D) and reconstituted it also into liposomes (i.e. phosphatidylcholine:cardiolipin). We treated the proteoliposomes with GD3–7 and observed that this molecule was able to induce the release of 4-MUP through the pore of ANT. The effect appeared to be specific for ANT, since it was inhibited by various doses of the endogenous ligands of ANT, ADP, and ATP (Fig. 3E). Moreover, GD3–7 was inactive on control liposomes without ANT (not shown). As the main isoform of ANT expressed in the rat heart is ANT1 [30], our results suggest that this ANT isoform is a functional target for GD3–7.

Having shown that only GD3–7, but not GD3 was able to form pores in the PTPC via an effect on ANT, we wondered if GD3–7 was detectable in cells during apoptosis. Hence we immunized mice with GD3–7 and used the antiserum for the detection of this GD3 derivative in the lipid extracts of cells. The antiserum did not bind to non-oxidized GD3 and the GD3-specific mAb R24 did not react with GD3–7 (Fig. 4A). Finally we analyzed the lipid fractions of the myeloid cell line HL-60 (Fig. 4B). In these cells GD3–7 was not present in the lipid extract of untreated cells but after induction of apoptosis by treatment with C2-ceramide, they showed a band with the mobility of our synthetically prepared GD3–7.

Discussion

In this study, we demonstrated for the first time, that in isolated mitochondria GD3–7 induces a PTPC-dependent swelling and depolarization, and that it is more potent than GD3 (Fig. 2). In contrast to GD3–7, acGD3 proved to be nontoxic on isolated mitochondria. This may be due to its resistance to oxidation. Moreover, using proteoliposome assays, a direct effect of GD3–7, but not of GD3, on PTPC proteins was observed. The GD3–7 effect was not seen in control vesicles without PTPC proteins or ANT indicating, that a specific ANT-GD3–7 interaction is responsible for the permeabilizing activity of GD3–7.

ANT is a bi-functional protein that exchanges cytosolic ADP against mitochondrial ATP in physiological conditions and can form a non-specific pore upon apoptosis induction. Although a genetic study in mice suggested that ANT would be non-essential for PT [31], its pharmacological conversion into a pore is considered as a potent means to induce MMP and cancer cell death [22, for review: 29]. In our study, the conversion of ANT into a pore by GD3–7 implies a conformational change that can be prevented by an excess of endogenous ligands of ANT, ADP, and ATP (Fig. 3). This suggests that conditions of low mitochondrial ATP production may favor the interaction of GD3–7 with ANT in cells.

Our study shows in addition the presence of GD3–7-aldehyde as a variant of the ganglioside GD3 only after apoptosis induction in HL-60 myeloid cells (Fig. 4B). The formation of GD3–7 in cells implies two main steps: (1) generation of GD3 from GM3, the most abundant ganglioside in human leucocytes, by a 2–8 sialyltransferase, and (2) oxidation of GD3 by ROS formed by the mitochondrial respiratory chain. This may explain the observation that GD3 is active at the cellular (not shown) the mitochondrial (Fig. 2) but not at the molecular level (Fig. 3).

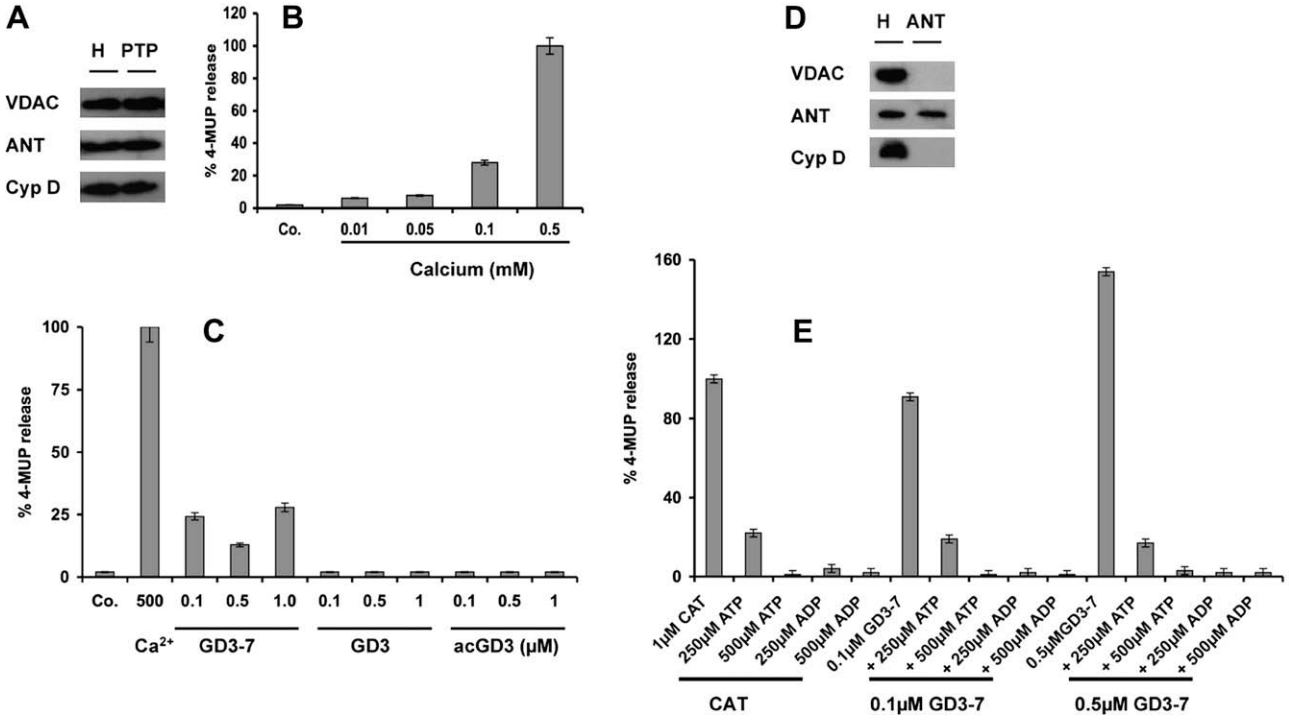

Fig. 3. Opening of the permeability transition pore (PTP) and the ANT pore in proteoliposomes. A. PTP was purified from rat brain and the presence of VDAC, ANT, and CypD in the enriched fraction was checked by Western-blotting after separation of proteins in SDS–PAGE (12%). H, brain homogenate; PTP, enriched fraction containing PTP proteins. (B) Calibration of the calcium response of PTP-containing liposomes. Proteoliposomes were incubated with various doses of Ca^{2+} for 1 h at 22 °C. Then, alkaline phosphatase and $MgCl_2$ were added and the 4-MU fluorescence was measured for 15 min. The maximal release induced by Ca^{2+} was normalized to 100% of 4-MUP release. (C) Effects of GD3 and its derivatives on PTP-containing liposomes. Proteoliposomes were incubated with Ca^{2+}, GD3–7, acGD3, GD3, or not (Co.) for 1 h at 37 °C and analyzed as in (B). The results are representative of three independent experiments performed in triplicate. (D) ANT was purified from rat heart and its absence of contamination by VDAC and CypD was checked by Western-blotting after SDS–PAGE separation (12%). (E) The effect of GD3–7 was evaluated on ANT-liposomes at the indicated doses at 20 °C. After 1 h of treatment of proteoliposomes, 4-MUP release was analyzed as in (B). The release of 4-MUP is calculated as percentage of the 100% release induced by CAT. Various doses of ATP and ADP were used to pretreat proteoliposomes for 30 min before GD3–7 and CAT addition. Results are representative of two independent experiments performed in triplicate.

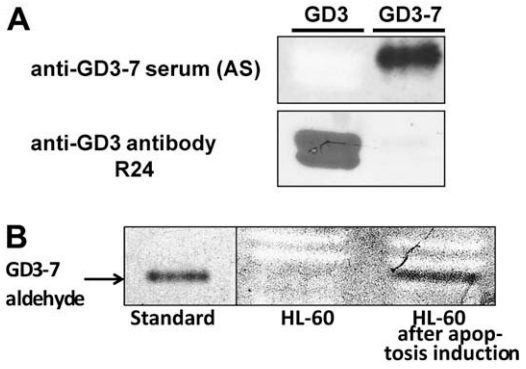

Fig. 4. Analysis of GD3–7 in apoptotic HL-60 cells. (A) Mutual exclusive binding of the GD3-specific antibody R24 and mouse antibody raised against GD3–7-aldehyde (GD3–7). GD3 and GD3–7 were separated on HPTLC plates in chloroform–methanol–water 120/70/17 for 35 min and immunostained with the GD3–7-specific serum and R24, respectively as described in Experimental Procedures. Left, 4.6 μg GD3; right, 0.2 μg GD3–7. (B) Detection of GD3–7 in apoptotic HL-60 cell extracts. Aliquots of desalted lipid extracts each corresponding to 1×10^7 cells were separated on HPTLC plates in chloroform–methanol–water 120/70/17 for 35 min and immunostained with anti-GD3–7 as described in Materials and methods. From left to right: about 10 ng GD3–7, lipid extracts of untreated and apoptotic HL-60 cells, respectively. Untreated HL-60 cells were 7% apoptotic and cells treated for 24 h with 30 μM C2-ceramide were 63% apoptotic. The experiment was repeated two times with similar results.

Acknowledgments

C.B. is supported by grants funded by Association pour la Recherche sur le Cancer (ARC), EGIDE, l'Agence Nationale pour la Recherche (ANR, ANR-08PCVI-0008-01), and l'Institut National pour le Cancer (INCa, 2008-1-PL BIO-04-CNRS ON1). We thank Ms Christine Gräfe and Ms Heidrun Gebauer for their help in preparing GD3-7 specific antisera. We are grateful to Britta Brügger for making the triple Quadrupole nanoESI-MS/MS available to us.

Appendix A. Supplementary data

Supplementary data associated with this article can be found, in the online version, at doi:10.1016/j.bbrc.2009.11.044.

References

[1] R. De Maria, L. Lenti, F. Malisan, F. ďAgostino, B. Tomassini, A. Zeuner, M.R. Rippo, R. Testi, Requirement for GD3 ganglioside in CD95- and ceramide-induced apoptosis, Science 277 (1997) 1652–1655.
[2] C. Garcia-Ruiz, A. Colell, A. Paris, J.C. Fernandez-Checa, Direct interaction of GD3 ganglioside with mitochondria generates reactive oxygen species followed by mitochondrial permeability transition, cytochrome c release, and caspase activation, FASEB J. 14 (2000) 847–858.
[3] A. Copani, D. Melchiorri, A. Caricasole, F. Martini, P. Sale, R. Carnevale, R. Gradini, M.A. Sortino, L. Lenti, R. De Maria, F. Nicoletti, Beta-amyloid-induced synthesis of the ganglioside GD3 is a requisite for cell cycle reactivation and apoptosis in neurons, J. Neurosci. 22 (2002) 3963–3968.
[4] B.S. Kristal, A.M. Brown, Apoptogenic ganglioside GD3 directly induces the mitochondrial permeability transition, J. Biol. Chem. 274 (1999) 23169–23175.
[5] F. Farina, F. Cappello, M. Todaro, F. Bucchieri, G. Peri, G. Zummo, G. Stassi, Involvement of caspase-3 and GD3 ganglioside in ceramide-induced apoptosis in Farber disease, Histochem. Cytochem. 48 (2000) 57–62.
[6] A. Colell, C. Garcia-Ruiz, J. Roman, A. Ballesta, J.C. Fernandez-Checa, Ganglioside GD3 enhances apoptosis by suppressing the nuclear factor-kappa B-dependent survival pathway, FASEB J. 15 (2001) 1068–1070.
[7] K. Woodfield, A. Ruck, D. Brdiczka, A.P. Halestrap, Direct demonstration of a specific interaction between cyclophilin-D and the adenine nucleotide translocase confirms their role in the mitochondrial permeability transition, Biochem. J. 336 (1998) 287–290.

[8] I. Marzo, C. Brenner, N. Zamzami, S.A. Susin, G. Beutner, D. Brdiczka, R. Remy, Z.H. Xie, J.C. Reed, G. Kroemer, The permeability transition pore complex: a target for apoptosis regulation by caspases and bcl-2-related proteins, J. Exp. Med. 187 (1998) 1261–1277.
[9] A. Colell, C. Garcia-Ruiz, M. Mari, J.C. Fernandez-Checa, Mitochondrial permeability transition induced by reactive oxygen species is independent of cholesterol-regulated membrane fluidity, FEBS Lett. 560 (2004) 63–68.
[10] M. Heidenheim, E.R. Hansen, O. Baadsgaard, CDw60, which identifies the acetylated form of GD3 gangliosides, is strongly expressed in human basal cell carcinoma, Br. J. Dermatol. 133 (1995) 392–397.
[11] G. Marquina, H. Waki, L.E. Fernandez, K. Kon, A. Carr, O. Valiente, R. Perez, S. Ando, Gangliosides expressed in human breast cancer, Cancer Res. 56 (1996) 5165–5171.
[12] D.A. Cheresh, R.A. Reisfeld, A.P. Varki, *O*-Acetylation of disialoganglioside GD3 by human melanoma cells creates a unique antigenic determinant, Science 225 (1984) 844–846.
[13] F. Malisan, L. Franchi, B. Tomassini, N. Ventura, I. Condo, M.R. Rippo, A. Rufini, L. Liberati, C. Nachtigall, B. Kniep, R. Testi, Acetylation suppresses the proapoptotic activity of GD3 ganglioside, J. Exp. Med. 196 (2002) 1535–1541.
[14] A.S. Blum, C.J. Barnstable, *O*-Acetylation of a cell-surface carbohydrate creates discrete molecular patterns during neural development, PNAS 84 (1987) 8716–8720.
[15] I. Nicoletti, G. Migliorati, M.C. Pagliacci, F. Grignani, C. Riccardi, A rapid and simple method for measuring thymocyte apoptosis by propidium iodide staining and flow cytometry, J. Immunol. Methods 139 (1991) 271–279.
[16] B. Kniep, C. Claus, J. Peter-Katalinic, D.A. Monner, W. Dippold, M. Nimtz, 7-*O*-Acetyl GD3 in human T-lymphocytes is detected by a specific T-cell-activating monoclonal antibody, J. Biol. Chem. 270 (1995) 30173–30180.
[17] R. Sandhoff, R. Geyer, R. Jennemann, C. Paret, E. Kiss, T. Yamashita, K. Gorgas, T.P. Sijmonsma, M. Iwamori, C. Finaz, R.L. Proia, H. Wiegandt, H.J. Gröne, Novel class of glycosphingolipids involved in male fertility, J. Biol. Chem. 280 (2005) 27310–27318.
[18] R. Sandhoff, S.T. Hepbildikler, R. Jennemann, R. Geyer, V. Gieselmann, R.L. Proia, H. Wiegandt, H.J. Gröne, Kidney sulfatides in mouse models of inherited glycosphingolipid disorders: determination by nano-electrospray ionization tandem mass spectrometry, J. Biol. Chem. 277 (2002) 20386–20398.
[19] R.H. McCluer, S.K. Gross, Biosynthesis of neutral glycosphingolipids in kidney slices from male and female mice, J. Lipid Res. 26 (1985) 593–599.
[20] U. Bethke, J. Müthing, B. Schauder, P. Conradt, P.F. Mühlradt, An improved semi-quantitative enzyme immunostaining procedure for glycosphingolipid antigens on high performance thin layer chromatograms, J. Immunol. Methods 89 (1986) 111–116.
[21] B. Kniep, P.F. Mühlradt, Monoclonal antibodies of the myeloid panel recognizing glycosphingolipids, in: A.J. McMichael (Ed.), Leukocyte Typing III, Oxford Univ. Press, London, 1987.
[22] A.S. Belzacq, H.L. Vieira, F. Verrier, G. Vandecasteele, I. Cohen, M.C. Prevost, E. Larquet, F. Pariselli, P.X. Petit, A. Kahn, R. Rizzuto, C. Brenner, G. Kroemer, Bcl-2 and Bax modulate adenine nucleotide translocase activity, Cancer Res. 63 (2003) 541–546.
[23] A. Tarze, A. Deniaud, M. Le Bras, E. Maillier, D. Molle, N. Larochette, N. Zamzami, G. Jan, G. Kroemer, C. Brenner, GAPDH, a novel regulator of the pro-apoptotic mitochondrial membrane permeabilization, Oncogene 26 (2007) 2606–2620.
[24] A.S. Belzacq-Casagrande, C. Martel, C. Pertuiset, A. Borgne-Sanchez, E. Jacotot, C. Brenner, Pharmacological screening and enzymatic assays for apoptosis, Front. Biosci. 14 (2009) 3550–3562.
[25] G. Beutner, A. Ruck, B. Riede, W. Welte, D. Brdiczka, Complexes between kinases, mitochondrial porin and adenylate translocator in rat brain resemble the permeability transition pore, FEBS Lett. 396 (1996) 189–195.
[26] C. Brenner, I. Marzo, H.L. De Araujo, G. Kroemer, Purification and liposomal reconstitution of permeability transition pore complex, Methods Enzymol. 322 (2000) 243–254.
[27] M. Crompton, E. Barksby, N. Johnson, M. Capano, Mitochondrial intermembrane junctional complexes and their involvement in cell death, Biochimie 84 (2002) 143–152.
[28] A.P. Halestrap, G.P. McStay, S.J. Clarke, The permeability transition complex: another view, Biochimie 84 (2002) 153–166.
[29] G. Kroemer, L. Galluzzi, C. Brenner, Mitochondrial membrane permeabilization and cell death, Physiol. Rev. 87 (2007) 99–163.
[30] A. Dorner, M. Olesch, S. Giessen, M. Pauschinger, H.P. Schultheiss, Transcription of the adenine nucleotide translocase isoforms in various types of tissues in the rat, Biochim. Biophys. Acta 1417 (1999) 16–24.
[31] J.E. Kokoszka, K.G. Waymire, S.E. Levy, J.E. Sligh, J. Cai, D.P. Jones, G.R. MacGregor, D.C. Wallace, The ADP/ATP translocator is not essential for the mitochondrial permeability transition pore, Nature 427 (2004) 461–465.